PAPER

The edge states properties of the topological insulator with fermion path nonanalyticity points located at the edge

To cite this article: A D Fedoseev 2020 *J. Phys.: Condens. Matter* **32** 215301

IOP Publishing Journal of Physics: Condensed Matter
J. Phys.: Condens. Matter **32** (2020) 215301 (8pp) https://doi.org/10.1088/1361-648X/ab73a9

The edge states properties of the topological insulator with fermion path nonanalyticity points located at the edge

A D Fedoseev

Kirensky Institute of Physics, Federal Research Center KSC SB RAS, Akademgorodok 50/38, 660036 Krasnoyarsk, Russia

E-mail: fad@iph.krasn.ru

Received 21 November 2019, revised 24 January 2020
Accepted for publication 6 February 2020
Published 27 February 2020

Abstract

The edge states properties of a finite-size 2D topological insulator (TI) with the open boundary conditions in both directions are studied. It is shown that fermion path nonanalyticity points appearing on the edge of finite-size TI cause a nonuniform edge state distribution along the TI edge. The character of this distribution depends substantially on the edge state's energy position in the bulk band gap. The edge state with the energy in the middle of the gap tends to be located in the corners between two nonparallel edges of the system, while the edge states with the energy close to the bulk band edge avoid the corners. The monotonic transition from one space distribution of the edge state wave function to another along the edge state's band is observed. The mentioned edge state's structure leads to the nonlinear current-voltage characteristic of the square-shaped TI with contacts connected with the corners of the device. It opens the possibility to control the current with the gate voltage and is useful for construction the nano-size devices. For the edge states with energy in the middle of a bulk gap, the vortex structure of the probability flux located near corners is found.

Keywords: topological insulator, edge states, electron transport

1. Introduction

Recently, topological insulators (TI), which is a new class of condensed matter with the dielectric gap in the bulk and gapless edge states, are attracting a lot of attention [1–7]. The edge states properties are of great attention because of their nontrivial properties [8–11]. For example, the TI without magnetic impurities are characterized by the absence of the backscattering of the edge states. The idea of topological protected edge states developed for solid-state physics was broaden to other systems, such as magnonic [12–14] and photonic crystals [15–17]. The investigation of the edge states are commonly carried out in the case of a semi-infinite system with only one surface. Generally, this approach appears to be sufficient to identify the energy and polarization characteristics. At once, the TI application in the micro- and nanoelectronic devices leads to the need of edge states properties investigation in the case of the open borders in all the directions.

The additional interest in the fully opened topological systems is connected with the prediction of the Majorana state in the 1D systems with superconducting coupling [18]. These zero energy states, which are predicted to emerge on the ends of nanowires or vortices for thin films, are expected to manifest non-Abelian quantum statistics [19]. The classification of topological phases for the case of noninteracting electrons was carried out in [20, 21]. In these papers, the authors considered the topological systems of a large size in order to be able to neglect the size effects.

At once, there are few studies of the edge states realization in small-size systems with open borders [22–29]. However, these studies show the appearance of size-effects in the TI and superconductors. The illustrative example of qualitative changing in properties of such systems induced by taking into account the open borders and finite system size was recently considered [22–24]. New lines in the parameter space corresponding to the presence of zero-energy modes were demonstrated in the case

of finite-size 1D models. The essential effect consists in the division of topological nontrivial phase, calculated in the case of the periodic boundary conditions, into the areas with the alternating fermion parity in the case of finite system with open borders. The zero-mode lines were shown to be the boundaries between the areas with opposite fermion parity. This leads to the presence of quantum phase cascade induced by external magnetic field in the case of quantum wires with the Rashba spin–orbit coupling and induced superconductivity. It is shown that this cascade manifests itself in the anomalous magnetocaloric effect behavior [23, 24].

In the case of 2D systems, the presence of two nonparallel edges leads to the appearance of the fermion path nonanalyticity points on the edge. There are two research guidelines of influence of these points on the topological system properties. The first guideline is connected with recently formulated the higher-order topological insulators concept [30]. These systems are gapped both in the bulk and the first-order edge spectrum, but contain the states located at the corner between two edges of the system and characterized by energy in the gaps. The special interest to the second-order edge states is caused by the existence of the Majorana corner states [31, 32] in the finite 2D second-order topological superconductors, which are protected by the energy gap.

The second guideline is connected with possible modification of the well-known edge states properties obtained in the case of the semi-infinite system with one open border [33]. The transition between the Majorana modes case and the chiral edge states case induced by the sides length ratio changing was shown for the 2D Kitaev model with the p-wave superconducting coupling. The same result was obtained for 2D system with Rashba spin–orbit coupling and induced superconductivity [34]. It was shown that the Majorana modes mixing in the corners of the system lead to their collapse.

The influence of the fermion nonanalyticity points on the system transport properties was recently studied in [35]. The authors carried out the analytical investigation of the transport properties in the case of the ring-shaped device built from two segments: a trivial and topological superconductors. However, the authors pointed out that such a system can hardly be realized in the experiment and should be replaced by square-shaped device. The numerical calculations for this geometry of the device showed that, in spite of the fact that there were no qualitative changes in the obtained results, the presence of the corners leads to quantitative changes. In the case of the square-shaped wire with the Rashba spin–orbit coupling, the corners induce a complete reflection from the device with the spin–orbit characteristic length and the square side length coincidence [36].

This study is carried out in the network of the latter guideline and devoted to the investigation of modification of well-known edge states properties in the case of finite-size 2D TI providing the presence of the fermion nonanalyticity points on its edges. This investigation is of great importance both for the experiment data interpretation, as well as for the search of new effects permitting the transport control in the nano-size devices. The calculation were performed in the framework of the Bernevig–Hughes–Zhang (BHZ) model.

2. Edge states properties of square-shaped 2D topological insulator

The BHZ Hamiltonian in the tight-binding approximation can be written as [37]

$$\begin{aligned}
&\mathcal{H}_{\mathrm{BHZ}} = \mathcal{H}_0 + \mathcal{T} + \mathcal{T}_{sp},\\
&\mathcal{H}_0 = -\varepsilon \sum_{f\sigma} c^{\dagger}_{f\sigma}\tau_z c_{f\sigma},\\
&\mathcal{T} = -t \sum_{\langle ff'\rangle\sigma} c^{\dagger}_{f'\sigma}\tau_z c_{f\sigma},\\
&\mathcal{T}_{sp} = -\mathrm{i}\alpha \sum_{f\sigma} \left[\sigma c^{\dagger}_{f+x\sigma}\tau_x c_{f\sigma} + c^{\dagger}_{f+y\sigma}\tau_y c_{f\sigma}\right] + \mathrm{h.c.},\\
&c^{\dagger}_{f\sigma} = \left(a^{\dagger}_{f\sigma},\ d^{\dagger}_{f\sigma}\right).
\end{aligned} \tag{1}$$

Here, the summation over f corresponds to the summation over the square sites, $\langle f'f\rangle$ is summation over the nearest neighbors, $f + x(y)$ is the site next to the f in $x(y)$ direction, τ_j—the Pauli matrix, $\sigma = \pm 1$ is the spin projection sign. The first term in the Hamiltonian is on-site energy of the s- and p-orbitals. The second term describes the hopping processes between orbitals of the same type. The last term describes the hopping processes between the orbitals of different types and takes into account the fact that the on-site spin–orbit coupling leads to the formation of $p_x + \mathrm{i}\sigma p_y$ orbitals and, consequently, the spin-dependent hopping phase factor [2, 38].

The eigenstates of the Hamiltonian (1) can be classified by σ, and may be written as

$$\Psi_{\sigma} = \sum_{f} \left[u_{f\sigma} a^{\dagger}_{f\sigma} + v_{f\sigma} d^{\dagger}_{f\sigma}\right] |0\rangle. \tag{2}$$

Square-shaped TI contains the edge states band with in-gap self energies as it does in the case of the periodic boundary conditions along one direction and open borders in another (cylinder geometry). The first difference from the latter case consist in the absence of degeneracy for the eigenstates with the same σ since they can not be independent any longer.

An important feature of BHZ model in the case of cylinder geometry is the connection between the spin projection of edge state and its velocity. As far as in the case of fully opened system the translational symmetry is absent in any direction, one should investigate the probability flux properties instead of velocity. In the tight-binding approximation [39], the components of the probability flow vector on the site f should be defined as

$$\begin{aligned}
j_{x(y)}(f) = \mathrm{Im}\Big(&u^{\dagger}_{f+x(y)}\widehat{H}_{f+x(y),f}u_f\\
&+ u^{\dagger}_f\widehat{H}_{f,f-x(y)}u_{f-x(y)}\Big)/\hbar,
\end{aligned} \tag{3}$$

where $u^{\dagger}_f = (u^{*}_{f\sigma},\ v^{*}_{f\sigma})$ is the row vector, $\widehat{H}$ is an appropriate 2×2 part of the Hamiltonian (1).

All the edge states in the square-shaped TI possess the probability flux circulating along the surface. The direction of this circulation depends on the spin projection σ and its value slightly differs from each other for different edge states. At once, there is a deviation for the edge states with energy level

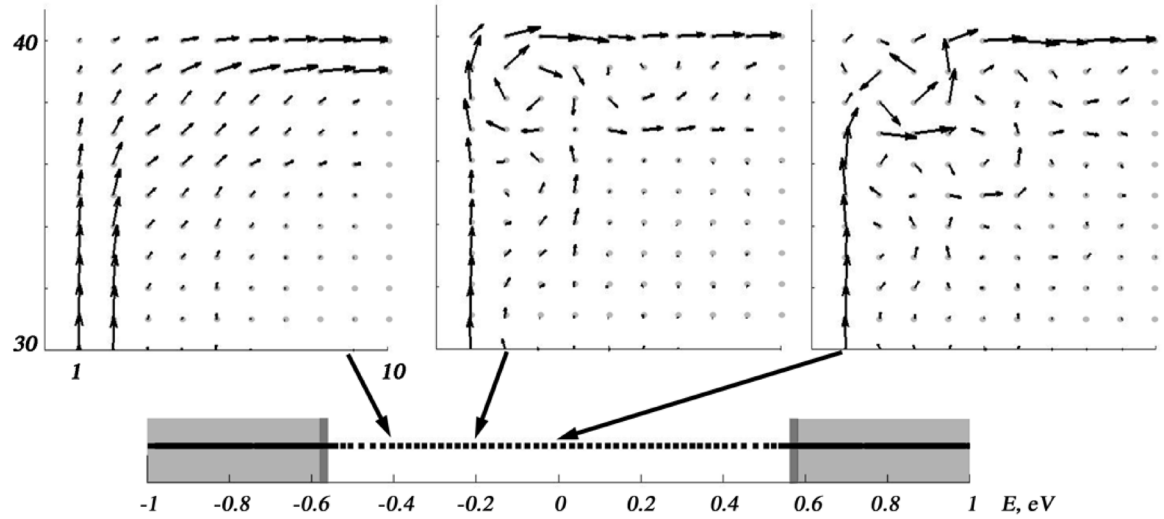

Figure 1. Typical probability flux spatial distribution in the corner of TI for the edge states with $\sigma = +1$ and different energies. The number of sites at the square side is $N = 40$. The bottom bar displays the allowed energies. Shaded areas mark the bulk bands and the space between them corresponds to the edge states band.

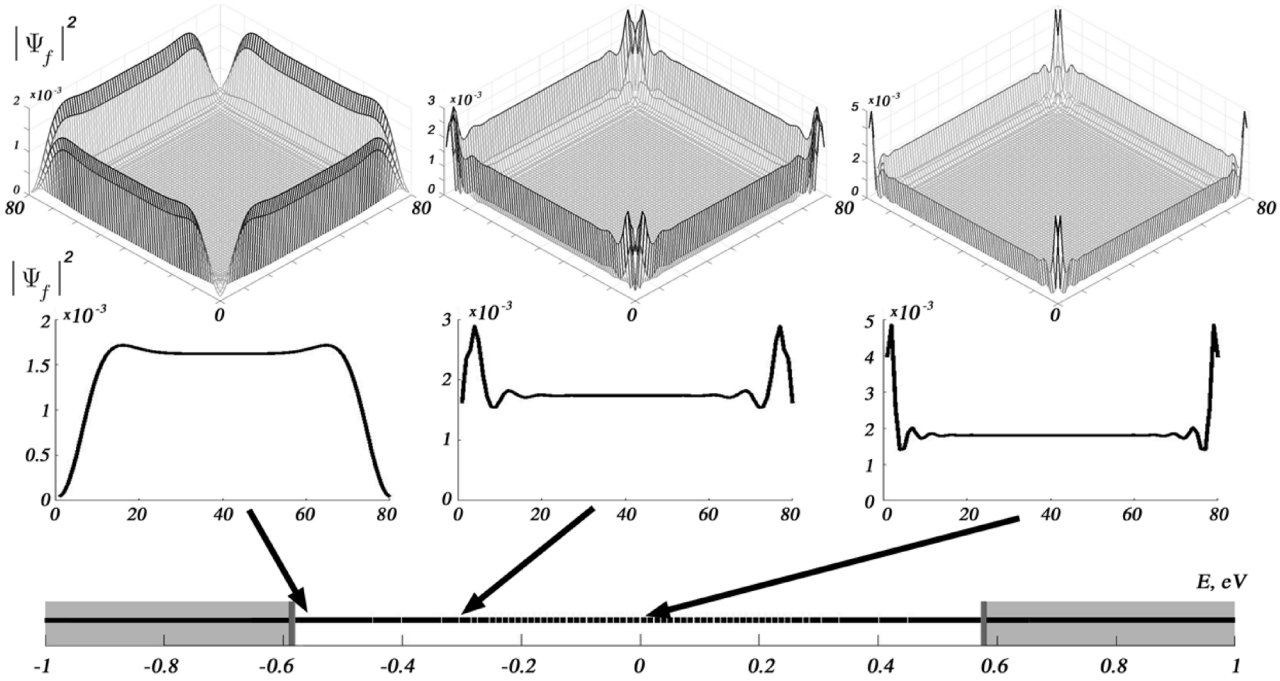

Figure 2. Spatial distribution of the edge states wave function amplitude. Left: edge state with the energy close to the edge states band edge. Center: edge state energy is equal to the quarter of the gap size. Right: edge state in the middle of the gap. Top figures represent the distribution on the whole square, bottom figures correspond to the distribution along the square side. Number of sites at the square side is $N = 80$. The bottom bar displays the allowed energies. Shaded areas mark the bulk bands and the space between them corresponds to the edge states band.

in the middle of the gap. Such states are characterized by the appearance of the vortexes in the corners of TI. The circulation direction of probability flux in the vortexes is opposite to that along the rest surface (figure 1).

These vortexes are connected with the non-monotonic edge states descent from the surface of TI into the bulk. As it was shown in [38, 40] this descent demonstrates the spatial oscillations. The size of the vortex is defined by period of the oscillations depending on the spin–orbit coupling constant α and the difference of the on-site energy ε for the s- and p-orbitals.

The presence of corners in the system leads to the dependence of the edge states on-site amplitude spatial modulation on the edge state energy. The edge states with the energy in the middle of the bulk band gap tend to be localized in the corners of the square. The edge states electron density in the corners continuously decreases with the edge state self energy moving away from the middle of the bulk gap, and the edge state amplitude spatial modulation changes to the opposite case: it vanishes for the edge states with energy close to the edge of edge states band (figures 2 and 3). At once, the wave

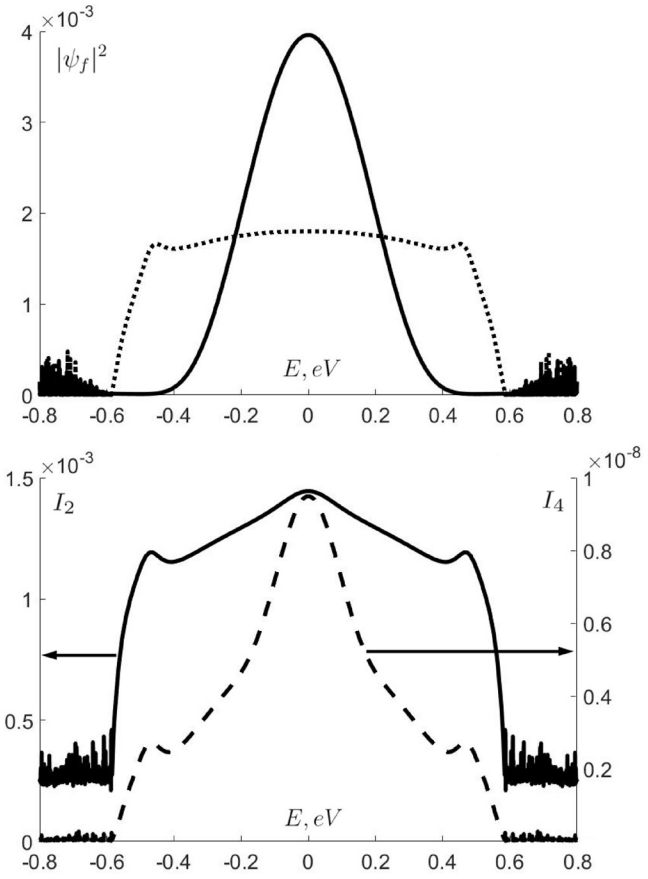

Figure 3. Top: wave function amplitude in the corners of the square (solid line) and at the middles of the square sides (dotted line) versus energy. Bottom: I_2 (solid line) and I_4 (dashed line) versus energy. $\varepsilon = 3,\ t = -1.2,\ \alpha = 0.3, N = 80$.

function amplitude at the middle of the square side remains almost the same for all the edge states. This feature should be expected to manifest itself in the transport properties of the square-shaped TI.

Commonly, it is useful to calculate the inverse participation ratio (IPR) [41, 42], which is defined as:

$$I_q(m) = \frac{\sum_f |\Psi_m(f)|^{2q}}{\left(\sum_f |\Psi_m(f)|^2\right)^q}, \tag{4}$$

where $\Psi_m(f)$ is the wave function with number m at the f site and q is usually set to be $q = 2$. The IPR is a constant for localized states ($I_q = 1$ if state is precisely localized at one site) and is $I_q = 1/V^{q-1}$ for the extended states in the system with V sites. As one can see in the bottom of figure 3, IPR well distinguishes the edge states and the bulk states and demonstrates the localization of the edge states with energy in the middle of the gap. Nevertheless, it fails to reveal the opposite effect: the vanishing of wave function in the corners of the square for the edge states with the energy close to the edge of the bulk band. At the same time this effect will be significant for the transport properties of the square-shaped TI.

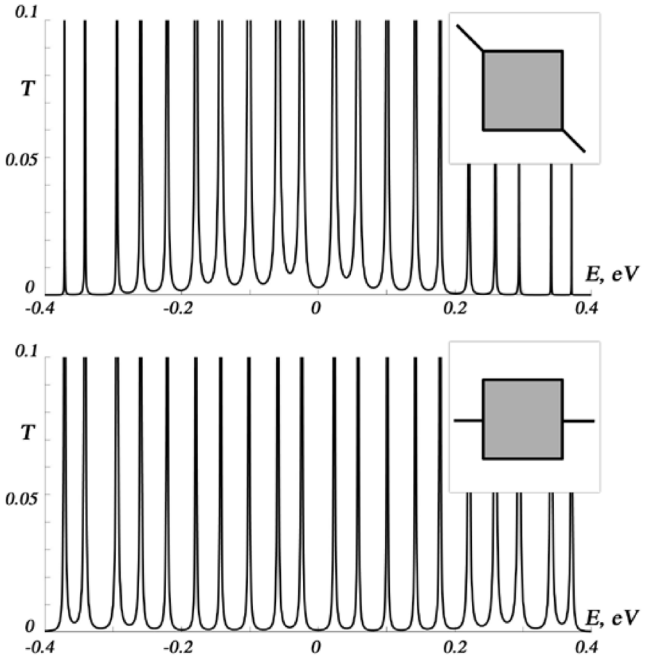

Figure 4. Transmission coefficient versus incident electron energy for the square-shaped TI device. Top: the contacts connected with the corners of square-shaped TI; Bottom: contacts connected with the middle of square sides. $\varepsilon = 3,\ t = -1.2,\ \alpha = 0.3, N = 20$.

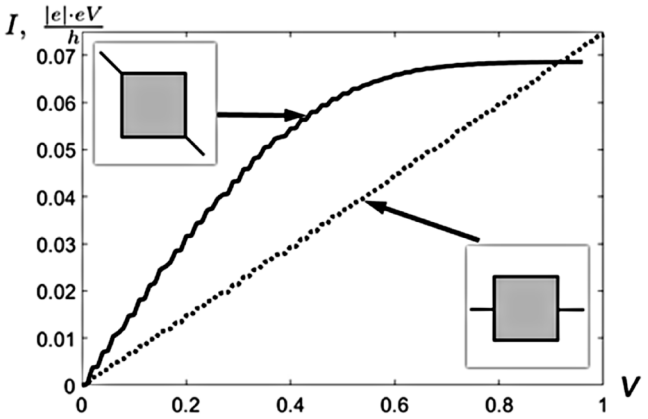

Figure 5. Current-voltage characteristics of the square-shaped TI. The solid line corresponds to the contacts connected with the corners of the device, the dashed line corresponds to the contacts connected with the middle of square sides. Wiggles originate from limited number of sites N and the low-temperature limit and the curves will smooth out in the case of sufficient great N.

3. Transport properties of square-shaped topological insulator

In this section, an observable consequence of the spatial modulation of the edge state amplitude in finite 2D TI will be shown. The transport properties of the system can be calculated using the Landauer–Büttiker approach. In this approach, the Shroedinger equation should be solved with the the Hamiltonian [43]

$$\widehat{H} = \widehat{H}_L + \widehat{H}_{LD} + \widehat{H}_{\mathrm{BHZ}} + \widehat{H}_{RD} + \widehat{H}_R,$$
$$\widehat{H}_L = t_L \sum_{n=-\infty,\sigma}^{-1} \left(c^\dagger_{n-1\sigma} c_{n\sigma} + c^\dagger_{n\sigma} c_{n-1\sigma} \right),$$
$$\widehat{H}_R = t_R \sum_{n=1,\sigma}^{\infty} \left(c^\dagger_{n+1\sigma} c_{n\sigma} + c^\dagger_{n\sigma} c_{n+1\sigma} \right),$$
$$\widehat{H}_{LD} = t_{LD} \sum_{\sigma} \left(c^\dagger_{-1\sigma} a_{f_L\sigma} + a^\dagger_{f_L\sigma} c_{-1\sigma} \right),$$
$$\widehat{H}_{RD} = t_{RD} \sum_{\sigma} \left(c^\dagger_{1\sigma} a_{f_R\sigma} + a^\dagger_{f_R\sigma} c_{1\sigma} \right). \quad (5)$$

Here, $\widehat{H}_{L,R}$ is the 1D-contact Hamiltonian, $\widehat{H}_{LD,RD}$ describes the electron tunneling between contacts and the device, where $a_{f_{L,R}}$ means the annihilation operator on the device site directly connected to the contacts. The approach assumes that the device has no other degrees of freedom except the electron ones.

The calculation of the transport characteristic reduces to the calculation of wave function in the electron scattering problem. This wave function can be written as

$$\Psi = \sum_{n=-\infty,\sigma}^{-1} w_{n\sigma} c^\dagger_{n\sigma}|0\rangle + \sum_{n=1,\sigma}^{\infty} z_{n\sigma} c^\dagger_{n\sigma}|0\rangle + \sum_{nm\sigma} \left(u_{f\sigma} a^\dagger_{f\sigma} + v_{f\sigma} d^\dagger_{f\sigma} \right)|0\rangle,$$
$$w_{n\sigma} = p_\sigma \mathrm{e}^{\mathrm{i}k_L n} + r_\sigma \mathrm{e}^{-\mathrm{i}k_L n}, \quad |p_\uparrow|^2 + |p_\downarrow|^2 = 1,$$
$$z_{n\sigma} = t_\sigma \mathrm{e}^{\mathrm{i}k_R n}, \quad (6)$$

where the expansion coefficients describe the incident and scattering wave in the case of left contact and transmitted wave in the right contact. Here, p_σ describes the incident electron spin polarization, and the vector $k_{L,R}$ has the measure of reciprocal interatomic distance.

The reflection and transmitting coefficient are defined by the reflecting and transmitting probability flux and incident flux ratio, correspondingly, as

$$R = \sum_\sigma |r_\sigma|^2, \quad T = \frac{t_R \sin k_R}{t_L \sin k_L} \sum_\sigma |t_\sigma|^2. \quad (7)$$

The spatial modulation of the wave function amplitude along the square side leads to the features in the transport properties of TI with fully opened borders (figure 4). In the case of the contacts connected with the corners of the device, the width of the transmission coefficient peaks differs substantially for the different energies in the gap (figure 4 on the top). The peaks corresponding to the excitation of the edge states, which have the energy in the middle of the gap, are wide, while that for the edge states, which have the energy close to the edge states band edge, are vanishingly narrow. This effect appears due to the transmission dependence of the coefficient peaks width on the corresponding one-electron state wave function amplitude at the sites connected with the contacts. On the contrary, in the case of the contacts connected with the middle of the square sides, the transmission peaks width is the same for different edge states energies (figure 4 on the bottom). It is connected with the weak wave function amplitude dependence on the edge state energy at the middle of the square sides.

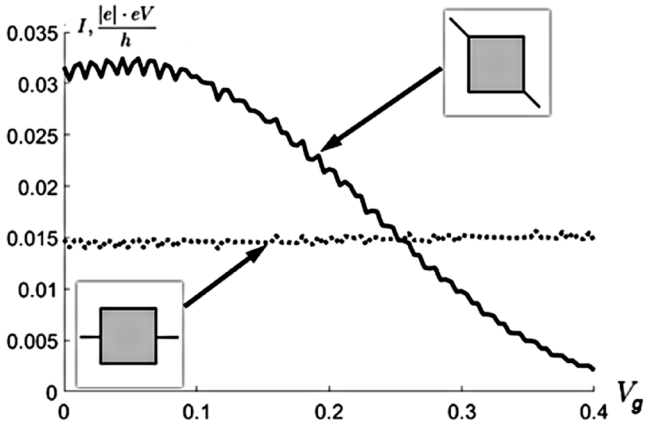

Figure 6. Current through the 2D TI versus gate voltage at $V = 0.2\ V$. The solid line corresponds to the contacts connected with the corners of the device, the dashed line corresponds to the contacts connected with the middle of square sides. The origin of the wiggles is the same as on the figure 5.

The current through the device connected with the 1D contacts in the Landauer–Bütticker approximation is given by

$$I = I_{LR} - I_{RL},$$
$$I_{LR} = \frac{2e}{L} \sum_k \frac{1}{\hbar} \left(\frac{\partial E}{\partial k} \right) T_{LR}(E) f_L(E),$$
$$I_{RL} = \frac{2e}{L} \sum_k \frac{1}{\hbar} \left(\frac{\partial E}{\partial k} \right) T_{RL}(E) f_R(E), \quad (8)$$

where T_{LR} and T_{RL} are the left-to-right and right-to-left transmission coefficients correspondingly, calculated with taking into account the additional term

$$\widehat{H}_V = \sum_{n=-\infty,\sigma}^{-1} eV_L c^\dagger_{n\sigma} c_{n\sigma} + \sum_{n=1,\sigma}^{\infty} eV_R c^\dagger_{n\sigma} c_{n\sigma}, \quad (9)$$

which the electric potential in the contacts. Here, $f_{L,R}(E) = f(E - \mu_{L,R})$ is the Fermi–Dirac distribution function. Passing from the summation on quasi-momentum to the integration over the energy, the expression for the current through the device takes the form [44]

$$I(V_L, V_R) = \frac{2e}{h} \int \mathrm{d}E \left[T_{LR} f_L(E) - T_{RL} f_R(E) \right]. \quad (10)$$

Here, the coincidence of the transmission coefficients for the different electron spin is taken into account.

With the transmission coefficient being the differential conductivity in the case of weak electric fields, the different current–voltage characteristics can be obtained depending on the contacts connection mode. The current–voltage characteristics is linear in the case of contacts connected with the middle of square sides, and it is significantly nonlinear for the contacts connected to the corner of the square-shaped TI (figure 5). The latter situation obtained in experiment could be wrongly explained as the density of the edge states dependence on the in-gap energy. In fact, this effect appears due to the dependence of the edge states amplitude at the corners of the system on its energy position in the gap.

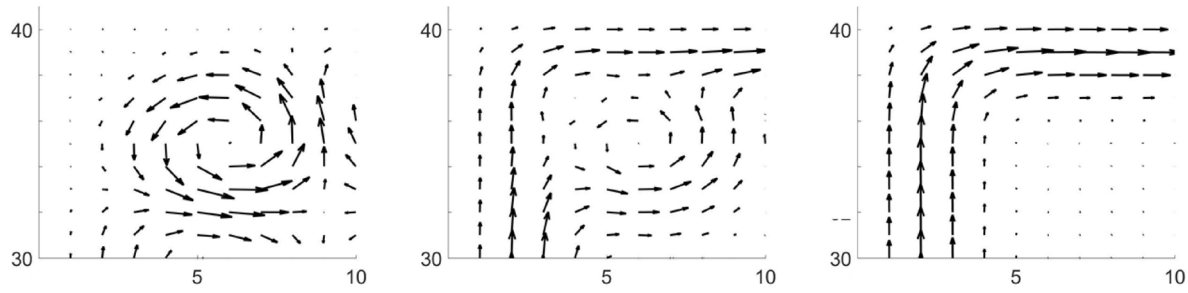

Figure A1. Probability flux spatial distribution in the corner of TI for the edge states with $\sigma = +1$ and the energy in the middle of the gap in the case of small interception of s and p initial bands $\varepsilon = 4.4$ and different spin-orbital coupling constant α. Left: $\alpha = 0.1$, center: $\alpha = 0.2$, right: $\alpha = 0.4$. The number of sites at the square side is $N = 40$.

Such a nonlinear current–voltage dependence opens the possibility to control the current with the gate voltage (one can read in [45] and experimental realization in supplemental materials in [46]). The typical current dependence on the gate voltage is shown on the figure 6.

4. Conclusion

The edge states properties are investigated in the case of the 2D TI with the fermion path nonanalyticity points on the edge arising in the fully opened geometry. The analysis was carried out in the tight-binding approximation in the framework of the BHZ model. It is shown that the bond between the edge state probability flux and its spin remains for the square-shaped TI in general. However, the presence of the fermion nonanalyticity points leads to the appearance of the probability flux vortexes located at the corners of the system for the edge states with the energy in the middle of the bulk band gap. The flux circulation in these vortexes is opposite to the general flux circulation direction.

Another consequence of the fermion nonanalyticity points is the edge states amplitude spatial distribution dependence on their energy. The edge state with the energy in the middle of the bulk gap tends to be localized in the corners of the 2D TI. The edge states band from the middle of the gap to its edges shows monotonic decreasing of the edge states amplitude at the corners and vanishing for the energy corresponding to the edge states band edge. The manifestation of this effect in the observable transport properties of the square-shaped TI was shown. So far as the wave function amplitude at the sites connected directly with the contacts defines the corresponding transmission coefficient peak width, this width decreases from the middle of the bulk gap to its edges in the case of the contacts connected with the corners, while it remains almost constant both in the case of the contacts connected to the middle of the square sides and in the case of cylindrical geometry. This feature leads to the fundamentally nonlinear current-voltage characteristics of the TI device. By turn, it opens the possibility to control the current with the gate voltage.

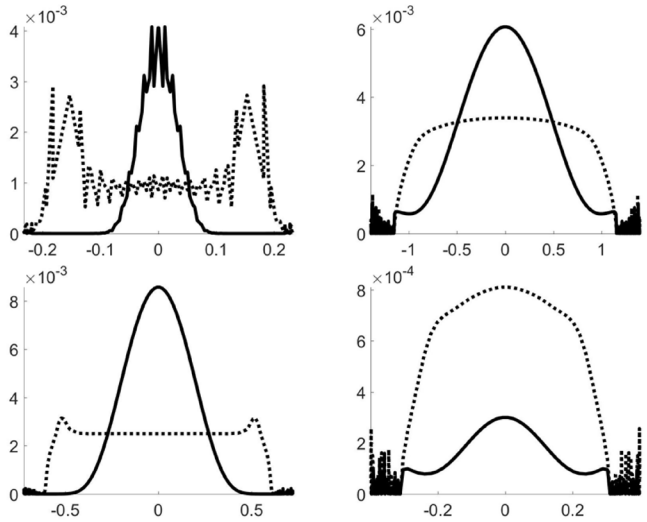

Figure A2. Wave function amplitude in the corners of the square (solid line) and at the middles of the square sides (dotted line) versus energy. Top-left: $\varepsilon = 3.0$, $\alpha = 0.1$; Top-right: $\varepsilon = 3.0$, $\alpha = 0.6$; Bottom-left: $\varepsilon = 2.4$, $\alpha = 0.3$; Bottom-right: $\varepsilon = 4.4$, $\alpha = 0.3$. The number of sites at the square side is $N = 60$.

Acknowledgments

The author thanks V V Val'kov and M M Korovushkin for the fruitful discussions and valuable remarks. The reported study was funded by the RAS Presidium program for fundamental research No. 32 'Nanostructures: physics, chemistry, biology and technology fundamentals', the Russian Foundation for Basic Research (project nos. 19-02-00348, 18-32-00443), Government of Krasnoyarsk Territory, Krasnoyarsk Regional Fund of Science to the research projects: 'Manifestation of Coulomb interactions and effects of restricted geometry in properties of topological edge states of nanostructures with spin–orbit coupling' (No. 18-42-243017), Council of the President of the Russian Federation for Support of Young Scientists and Leading Scientific Schools (project no. MK-3722.2018.2).

Appendix. The effect of the parameters on the edge states properties of square-shaped TI

We have two energy parameters to vary in our model: the spin–orbit coupling constant α and the difference of the on-site energy ε for the s- and p-orbitals. In the $\alpha \ll |t|$ limit the spin–orbit constant is responsible for the gap size $\Delta \sim \alpha$ and the localization length of the edge states, which is $L_{\mathrm{loc}} \sim |t/\alpha|$ for the edge states with the energy in the middle of the gap. In

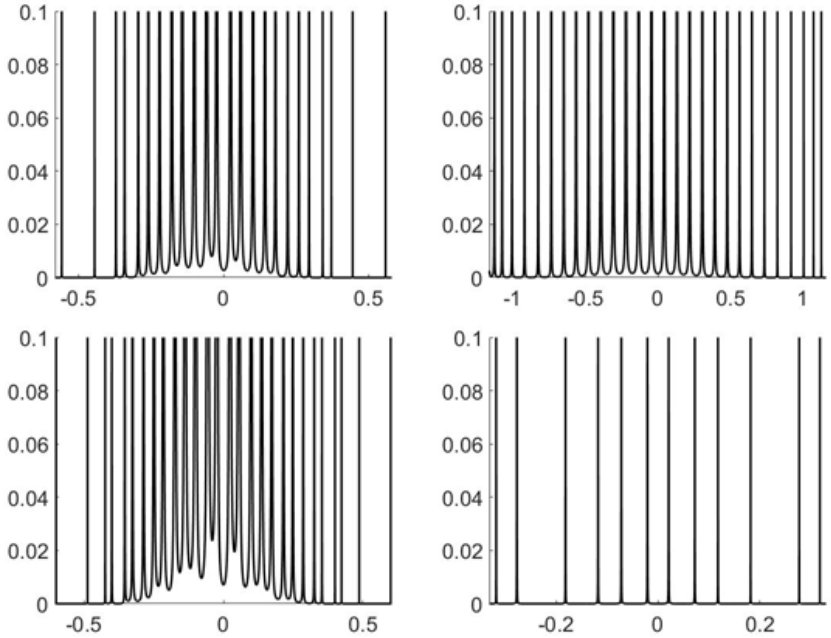

Figure A3. Transmission coefficient versus incident electron energy for the square-shaped TI device in the case of the contacts connected with the corners. Top-left: $\varepsilon = 3.0$, $\alpha = 0.3$; top-right: $\varepsilon = 3.0$, $\alpha = 0.6$; bottom-left: $\varepsilon = 2.4$, $\alpha = 0.3$; bottom-right: $\varepsilon = 4.4$, $\alpha = 0.3$. The number of sites at the square side is $N = 20$.

the same limit the on-site orbital splitting ε, which determines the interception of the initial s and p bands, is responsible for the oscillation period of the edge states descending.

One can obtain a larger flux probability vortex size in the corner of the square, mentioned in the section 2, by taking $\varepsilon \to 4|t|$ (figure A1). In this case the size of such vortex is determined as:

$$L \approx \frac{\pi}{2\sqrt{1 - |\varepsilon/4t|}}. \tag{A.1}$$

At the same time the spin-orbital constant effects in localization of the edge states on the edge of the system, so the increasing of α leads to the suppression of the vortex and restoring of the 'right' direction of the probability flux in the corners (figure A1).

While the appearance of the vortex structure and its size in the probability flux of the edge state with the energy in the middle of the gap is sensitive to the parameters of the system, the effect of changing of edge state spatial distribution character with changing of its energy is insensitive. The electron density in the corners almost monotonically decrease along the edge states band from the middle of the bulk band gap to its edge, although it does not vanish in the case of rather large α (figure A2). At the same time the wave function amplitude in the corners differs for different parameter sets according to the spin–orbit coupling efforts to put the edge state amplitude maximum on the site located on the edge, while the oscillations, defined by ε, attempt to move it away from the edge. It results in the different peak width in the dependence of transmission coefficients on incident electron energy for the square-shaped TI device (figure A3) for different sets of parameters. However, the qualitative effect consisting in the dependence of the width of the transmission coefficient peaks on the incident electron energy remains.

ORCID iDs

A D Fedoseev https://orcid.org/0000-0002-3073-2101

References

[1] Volkov B A and Pankratov O A 1985 *JETP Lett.* **42** 178
[2] Bernevig B A, Hughes T L and Zhang S C 2006 *Science* **314** 1757
[3] Fu L, Kane C L and Mele E J 2007 *Phys. Rev. Lett.* **98** 106803
[4] Zhang Y-Y, Wang X-R and Xie X C 2012 *J. Phys.: Condens. Matter* **24** 015004
[5] Ren Y, Qiao Z and Niu Q 2016 *Rep. Prog. Phys.* **79** 066501
[6] Tarasenko S A 2018 *Phys.—Usp.* **61** 1026B
[7] Rachel S 2018 *Rep. Prog. Phys.* **81** 116501
[8] Kane C L and Mele E J 2005 *Phys. Rev. Lett.* **95** 226801
[9] Hasan M Z and Kane C L 2010 *Rev. Mod. Phys.* **82** 3045
[10] Hasan M Z, Xu S-Y and Bian G 2015 *Phys. Scr.* **164** 014001
[11] Pankratov A O 2019 *Phys.—Usp.* **61** 1116
[12] Zhang L, Ren J, Wang J-S and Li B 2013 *Phys. Rev.* B **87** 144101
[13] Owerre S A 2017 *Sci. Rep.* **7** 6931
[14] Pirmoradian F, Rameshti B Z, Miri M and Saeidian S 2018 *Phys. Rev.* B **98** 224409
[15] Haldane F D M and Raghu S 2008 *Phys. Rev. Lett.* **100** 013904
[16] Downing C A, Sturges T J, Weick G, Stobinska M and Martin-Moreno L 2019 *Phys. Rev. Lett.* **123** 217401
[17] Ozawa T *et al* 2019 *Rev. Mod. Phys.* **91** 015006
[18] Kitaev A Yu 2001 *Phys.—Usp.* **44** 131
[19] Stanescu T D and Tewari S 2013 *J. Phys.: Condens. Matter* **25** 233201

[20] Schnyder A P, Ryu S, Furusaki A and Ludwig A W W 2008 *Phys. Rev.* B **78** 195125
[21] Kitaev A Yu 2009 *AIP Conf. Proc.* **1134** 22
[22] Hegde S, Shivamoggi V, Vishveshwara S and Sen D 2015 *New J. Phys.* **17** 053036
[23] Val'kov V V, Mitskan V A and Shustin M S 2017 *JETP Lett.* **106** 798
[24] Val'kov V V, Mitskan V A and Shustin M S 2019 *JETP* **129** 426
[25] Chen R and Zhou B 2016 *Chin. Phys.* B **25** 067204
[26] Hsu M C, Lin Y-C and Chang C-R 2015 *J. Appl. Phys.* **118** 043909
[27] Hattori K 2015 *J. Phys. Soc. Japan* **84** 044701
[28] Ortiz L, Molina R A, Platero G and Lunde A M 2016 *Phys. Rev.* B **93** 205431
[29] Valkov V V, Zlotnikov A O, Fedoseev A D and Shustin M S 2017 *J. Magn. Magn. Mater.* **440** 37
[30] Benalcazar W A, Bernevig B A and Hughes T L 2017 *Science* **357** 61
[31] Wang Q, Lie C-C, Lu Yu-M and Zhang F 2018 *Phys. Rev. Lett.* **121** 186801
[32] Zhu X 2018 *Phys. Rev.* B **97** 205134
[33] Potter A C and Lee P A 2010 *Phys. Rev. Lett.* **105** 227003
[34] Sedlmayr N, Aguiar-Hualde J M and Bena C 2016 *Phys. Rev.* B **93** 155425
[35] Lee M, Khim H and Choi M-S 2014 *Phys. Rev.* B **89** 035309
[36] Val'kov V V and Fedoseev A D 2017 *JETP Lett.* **106** 302
[37] Begue F, Pujol P and Ramazashvili R 2018 *JETP* **126** 90
[38] Dang X, Burton J D, Kalitsov A, Velev J P and Tsymbal E Y 2014 *Phys. Rev.* B **90** 155307
[39] Datta S 2005 *Quantum Transport: Atom to Transistor* (New York: Cambridge University Press) p 150
[40] Fedoseev A D 2019 *JETP* **128** 125
[41] Calixto M and Romera E 2015 *J. Stat. Mech.* **2015** 06029
[42] Murphy N C, Wortis R and Atkinson W A 2011 *Phys. Rev.* B **83** 184206
[43] Val'kov V V and Aksenov S V 2011 *JETP* **113** 266
[44] Datta S 1995 *Electronic Transport in Mesoscopic Systems* (New York: Cambridge University Press) p 53
[45] Alhassid Y 2000 *Rev. Mod. Phys.* **72** 895
[46] Piatrusha S U, Tikhonov E S, Kvon Z D, Mikhailov N N, Dvoretsky S A and Khrapai V S 2019 *Phys. Rev. Lett.* **123** 056801